Nature Materials 11 (2012) 690-693

$Al_{13}Fe_4$ as a low-cost alternative for palladium in heterogeneous hydrogenation

M. Armbrüster[1]*, K. Kovnir[1], M. Friedrich[1], D. Teschner[2], G.Wowsnick[1], M. Hahne[3], P. Gille[3], L. Szentmiklósi[4], M. Feuerbacher[5], M. Heggen[5], F. Girgsdies[2], D. Rosenthal[2], R. Schlögl[2] and Yu. Grin[1]

[1]Max-Planck-Institut für Chemische Physik fester Stoffe, Nöthnitzer Str. 40, 01187 Dresden, Germany
[2]Fritz-Haber Institute of the Max Planck Society, Department of Inorganic Chemistry, Faradayweg 4-6, 14195 Berlin, Germany
[3]Ludwig-Maximilians-University Munich, Department of Earth and Environmental Sciences, Theresienstr. 41, 80333 Munich, Germany
[4]Centre for Energy Research, Hungarian Academy of Sciences, PO Box 49, H-1525 Budapest, Hungary
[5]Forschungszentrum Jülich GmbH, Institute for Solid State Research, 52425 Jülich, Germany.

* Corresponding author: e-mail marc.armbrüster@cpfs.mpg.de,

Received 12 January 2012; Accepted 02 May 2012; Published online 10 June 2012

Keywords: $Al_{13}Fe_4$, selective hydrogenation, in situ stability, active-site isolation, noble-metal free, intermetallic compound

Replacing noble metals in heterogeneous catalysts by low-cost substitutes has driven scientific and industrial research for more than 100 years. Cheap and ubiquitous iron is especially desirable, because it does not bear potential health risks like, for example, nickel. To purify the ethylene feed for the production of polyethylene, the semi-hydrogenation of acetylene is applied (80×10^6 tons per annum; [1,2,3]). The presence of small and separated transition-metal atom ensembles (so-called site-isolation), and the suppression of hydride formation are beneficial for the catalytic performance[4,5,6]. Iron catalysts necessitate at least 50 bar and 100 °C for the hydrogenation of unsaturated C–C bonds, showing only limited selectivity towards semi-hydrogenation[7-13]. Recent innovation in catalytic semi-hydrogenation is based on computational screening of substitutional alloys to identify promising metal combinations using scaling functions[14] and the experimental realization of the site-isolation concept employing structurally well-ordered and *in situ* stable intermetallic compounds of Ga with Pd[15-19]. The stability enables a knowledge-based development by assigning the observed catalytic properties to the crystal and electronic structures of the intermetallic compounds[20,21]. Following this approach, we identified the low-cost and environmentally benign intermetallic compound $Al_{13}Fe_4$ as an active and selective semi-hydrogenation catalyst. This knowledge-based development might prove applicable to a wide range of heterogeneously catalysed reactions.

On the iron-poor side of the Al–Fe phase diagram, several structurally complex intermetallic compounds with more than 100 atoms in the unit cell are formed. In monoclinic $Al11_3Fe_4$[22], the iron atoms are either solely coordinated by aluminium or arranged in Fe–Al–Fe groups located in the cavities of the three-dimensional Al framework, resulting in a complete encapsulation of the potential active transition-metal sites by aluminium atoms, thus, following the site-isolation concept (Fig. 1a). Single-crystalline $Al_{13}Fe_4$ was synthesized from the elements[23] (Supplementary Fig. S1). Using the same sample for catalytic reactor experiments and ultrahigh vacuum (UHV) stability studies, in the form of powdered material and single-crystalline slices, respectively, allows reducing the so-called materials gap[24] between reactor and UHV investigations in this study to a minimum. This enables the most meaningful comparison of the results obtained in the different pressure regimes. Catalytic tests on 20 mg of unsupported $Al_{13}Fe_4$ in an industry-like ethylene feed containing 0.5% C_2H_2 result right from the start in high conversion and a very high ethylene-selectivity of 81–84% (Fig. 1b). Selectivity towards C4 compounds formed by C–C coupling amounted to 7–10% and higher hydrocarbons were not observed. Only negligible amounts of carbonaceous deposits were detected

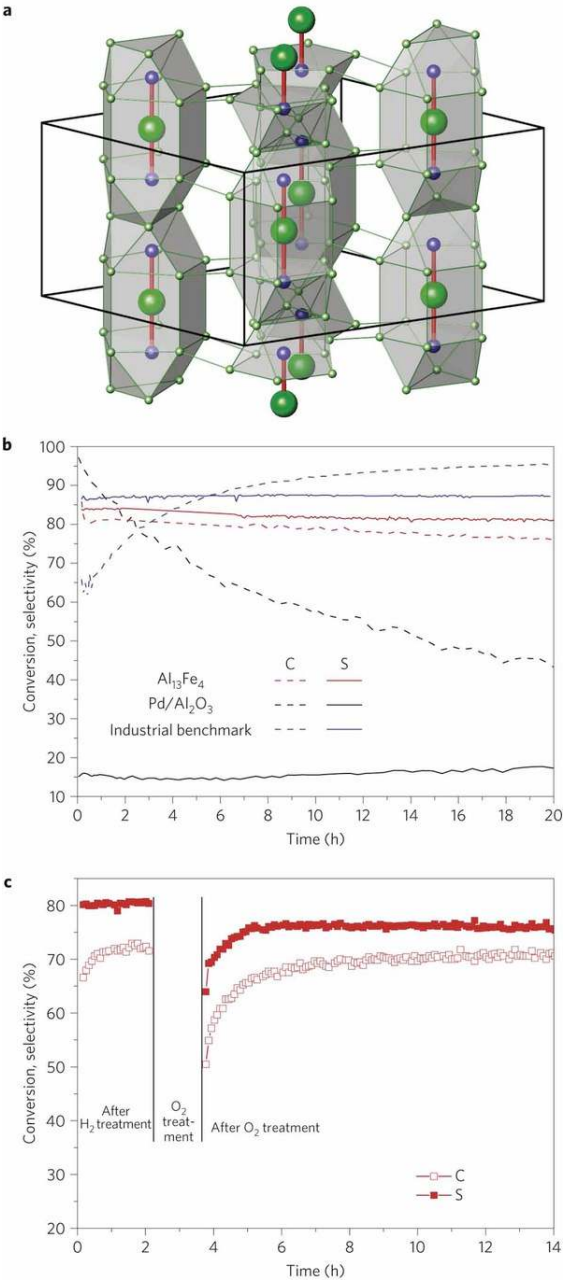

Fig. 1a, Unit cell of $Al_{13}Fe_4$ emphasizing the structurally isolated Fe–Al–Fe units (Al, green; Fe, blue). **b**, Conversion (C) and selectivity (S) to ethylene of unsupported $Al_{13}Fe_4$, 5 wt% Pd/Al_2O_3 and an industrial benchmark catalyst in the semi-hydrogenation of acetylene over 20 h time on stream (reaction conditions: 0.5% C_2H_2, 5% H_2, 50% C_2H_4 in He, 30 ml min^{-1} total flow, 200 °C). **c**, Catalytic properties of $Al_{13}Fe_4$ after treatment in hydrogen and oxygen.

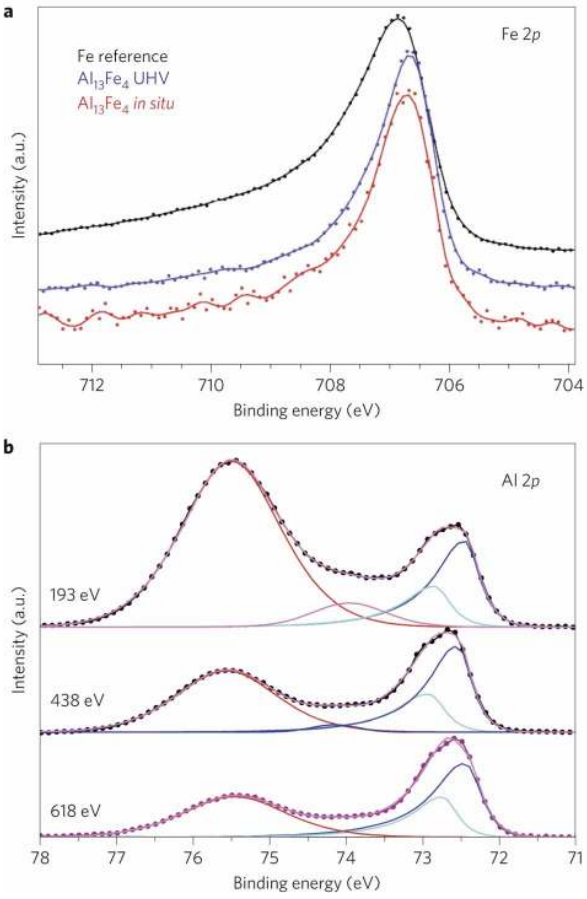

Fig. 2a, Fe 2*p* XPS spectra of the single-crystalline (010) surface of $Al_{13}Fe_4$ and elemental Fe foil as a reference with 860 and 900 eV photon energy, respectively. **b**, XPS spectra of the Al 2*p* region corresponding to inelastic mean free paths of 6.6, 11.3 and 14.7 nm[30] from top to bottom.

by Raman spectroscopy and temperature-programmed oxidation measurements after up to 160 h time on stream in accordance with the carbon balance of 99–100% determined from the effluent gas (for details see Supplementary Information). In contrast to the very active commercial 5 wt% Pd/Al_2O_3, $Al_{13}Fe_4$ shows high stability and only 6% lower selectivity towards ethylene than an industrial benchmark catalyst. Whereas the benchmark catalyst has been highly optimized for this application, the $Al_{13}Fe_4$ is just the material itself without any support or engineering applied for optimization. Therefore, we expect that further optimization of $Al_{13}Fe_4$ in terms of supporting the material or adjusting the particle size may lead to an even better performance.

With two further tests we verified the active role of the intermetallic surface. First, $Al_{13}Fe_4$ was subjected to a reductive H_2 treatment after 20 h time on stream. The selectivity was not influenced by the reductive treatment and the initial activity was restored within 1 h (Fig. 1c). In contrast, activity and selectivity suffered significantly by treating the catalyst in O_2 at 200 °C. It takes several hours until the activity recovers, and the selectivity does not reach the value of the untreated catalyst, revealing detrimental and irreversible changes on the surface. Second, the surface of $Al_{13}Fe_4$ is slightly oxidized (see below) by handling in air, which may lead to Al_2O_3-supported Fe nanoparticles on the intermetallic surface. Therefore, we tested fine and unsupported iron powder as well as a 4 wt% Fe/Al_2O_3 under identical conditions after a reductive pre-treatment, but found both to be catalytically inactive for the semi-hydrogenation of acetylene.

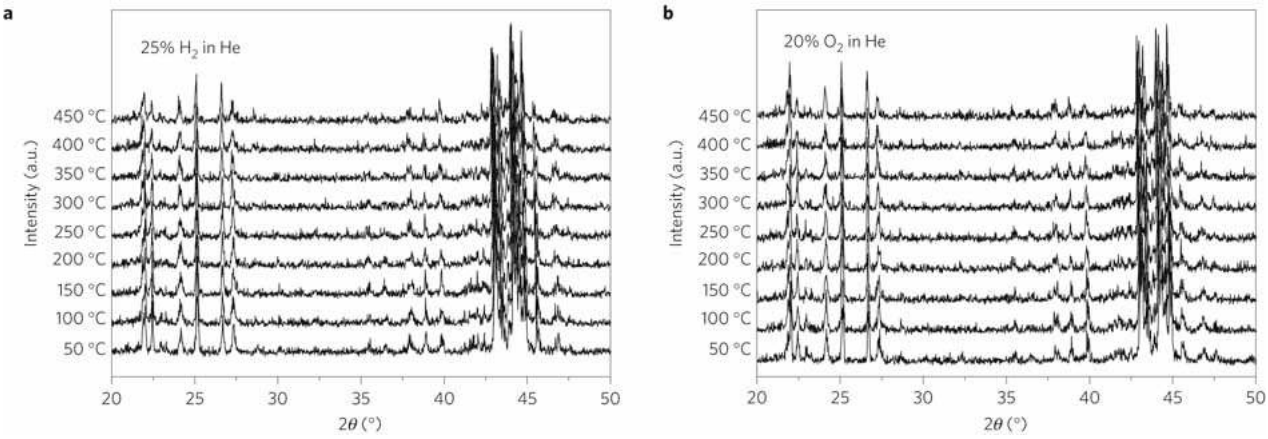

Fig. 3, Temperature-dependent X-ray powder diffraction patterns of $Al_{13}Fe_4$ in 25% H_2 (a) and 20% O_2 (b) in helium.

To unambiguously establish the catalytic role of $Al_{13}Fe_4$, the stability of the compound under reaction conditions was investigated. The surface of $Al_{13}Fe_4$ was characterized by X-ray photoelectron spectroscopy (XPS). Comparison of the valence-band XPS spectra of a (010)-oriented single crystal of $Al_{13}Fe_4$ with catalytically inactive elemental Fe indicates only a slight modification of the electronic structure around the Fermi energy (Supplementary Fig. S5). Fe 2*p* core-level spectra in Fig. 2 reveal only one signal attributed to $Al_{13}Fe_4$ with fine differences to elemental iron (small shift, decreased half-width, reduced asymmetry) and exclude the presence of additional Fe nanoparticles that would broaden the Fe 2*p* peak towards higher binding energy. The differences are typical for intermetallic compounds of transition metals and main group elements with isolated transition-metal atoms, for example Pd in GaPd[17], and are attributed to the altered electronic structure, leading to a different screening of the core hole. The signals in the Al 2*p* region of the XPS spectra are assigned to three Al-containing species (Fig. 2b). $Al_{13}Fe_4$ gives rise to a contribution that is split into two signals by spin–orbit coupling at 72.5 and 72.9 eV. In addition, the signals of Al_2O_3 (75.5 eV) and of another oxidized Al compound at 74.0 eV are detected. Both signals from the oxidized species monotonically decrease with increasing information depth, resulting in a hypothetically perfect Al_2O_3 layer with a thickness of only 6.9 Å[25], whereas the signals associated with $Al_{13}Fe_4$ increase in intensity. The partial oxidation and the absence of elemental iron on the surface can be explained by the small, but significant, homogeneity range of $Al_{13}Fe_4$, which allows withdrawing the Al partly without destroying the compound. As the single crystal showed the expected sharp low-energy electron diffraction pattern for $Al_{13}Fe_4$, the intermetallic surface can only be covered partly by the oxide. Calculating the elemental ratios of the Al, Fe and O signals shows that Al_2O_3 and $Al_{13}Fe_4$ are close to their nominal composition. Investigating the material under acetylene hydrogenation conditions by high-pressure XPS, the electronic states remained widely unaffected (Fig.2), indicating an unaltered surface, and thus the presence of $Al_{13}Fe_4$ under reaction conditions. Carbon depth profiling of $Al_{13}Fe_4$ implied only surface carbon, as opposed to elemental Pd catalysts where subsurface carbon plays a crucial role for the selectivity[26].

To demonstrate the in situ bulk stability of $Al_{13}Fe_4$, the compound was studied by bulk-sensitive techniques. In situ X-ray powder diffraction in reducing or oxidizing atmospheres revealed the stability of the bulk structure up to temperatures of 450 °C (Fig. 3). The stability in a reducing atmosphere was also corroborated by combined differential thermal analysis and thermal gravimetric measurements (Supplementary Fig. S6). Being very sensitive to hydride formation, prompt gamma activation analysis (PGAA) was applied to $Al_{13}Fe_4$ in a mixture of propyne, ethylene and hydrogen in 1:5:7 ratios at 200 °C. Whereas it shows a high selectivity of 90% towards propylene, $Al_{13}Fe_4$ did not dissolve hydrogen in the bulk. Even in a pure hydrogen atmosphere, no hydrogen uptake was detected. Combination of surface- and bulk-sensitive methods clearly shows that $Al_{13}Fe_4$ does not change under reaction conditions, and allows unambiguously assigning the catalytic properties to the intermetallic compound.

The stability of $Al_{13}Fe_4$ under reaction conditions is due to the covalent interactions revealed by quantum chemical calculations within the electron localizability/electron density approach[27]. In combination with the low iron content, this results in highly stable isolated iron-containing ensembles. This structural motif is in strong contrast to elemental iron, where the large number of neighbouring Fe atoms leads to strong adsorption of the reactants, resulting in the characteristic activity of elemental Fe in C–C coupling reactions such as Fischer–Tropsch catalysis and carbon nanotube synthesis[28,29]. In $Al_{13}Fe_4$, the structural situation resembles that of the Ga-only coordinated Pd atoms in the intermetallic compound GaPd, which proved to be an excellent semi-hydrogenation catalyst[15]. Similar investigations on the intermetallic compound $Al_{13}Co_4$ re-

sulted in comparable properties, showing that $Al_{13}Fe_4$ is not an exceptional case.

Guided by the site-isolation concept, the noble-metal-free and environmentally benign intermetallic compound $Al_{13}Fe_4$ was identified as a potent and low-cost replacement for Pd-based hydrogenation catalysts. The in situ stable intermetallic compound exhibits excellent catalytic properties, which are assigned to the combination of site-isolation and the alteration of the electronic structure by the chemical bonding. Our results show the possibility to tailor the catalytic properties of cheap 3d transition metals by formation of intermetallic compounds with abundant p-elements—an approach that should be broadly applicable in heterogeneous catalysis. Further work will be performed to reveal and understand the underlying elementary reaction steps as well as to test the transferability to other reactions.

Acknowledgement

We thank G. Auffermann for chemical analysis, R. Wagner for the UHV preparation of the single crystals and S. Hoffmann as well as E. Kitzelmann for in situ differential thermal analysis and thermal gravimetric measurements. The European Network of Excellence on 'Complex Metallic Alloys', contract No. NMP3-CT-2005-500140, the EU FP7 NMI3 Access Programme and the NAP VENEUS grant (OMFB-00184/2006) are acknowledged for supporting this work in part and the *in situ* PGAA measurements, respectively. Beam time for *in situ* XPS measurements was provided by the Helmholtz-Zentrum Berlin für Materialien und Energie GmbH (ID 2010_1_90734) and we thank the team of the ISIS-PGM beamline for continuous support. The European Centre for Development of Alloys and Compounds (C-MAC) nurtured this publication by providing a networking platform.

References

1. Piringer, O. G. & Baner, A. L. *Plastic Packaging: Interactions with Food and Pharmaceuticals* 2nd edn (Wiley, 2008).
2. Borodzinski, A. & Bond, G. C. Selective hydrogenation of ethyne in ethene-rich streams on palladium catalysts. Part 1. Effect of changes to the catalyst during reaction. *Catal. Rev. Sci. Engin.* **48**, 91–144 (2006).
3. Borodzinski, A. & Bond, G. C. Selective hydrogenation of ethyne in ethene-rich streams on palladium catalysts, Part 2: Steady-state kinetics and effects of palladium particle size, carbon monoxide, and promoters. *Catal. Rev. Sci. Eng.* **50**, 379–469 (2008).
4. Ahn, I. Y., Lee, J. H., Kim, S. K. & Moon, S. H. Three-stage deactivation of Pd/SiO_2 and $Pd–Ag/SiO_2$ catalysts during the selective hydrogenation of acetylene. *Appl. Catal. A* **360**, 38–42 (2009).
5. Khan, N. A., Shaikhutdinov, S. & Freund, H-J. Acetylene and ethylene hydrogenation on alumina supported Pd–Ag model catalysts. *Catal. Lett.* **108**, 159–164 (2006).
6. Derouane, E. G. Second European Symposium on Catalysis by Metals. Multimetallic catalysts in synthesis and transformation of hydrocarbons: Concluding remarks, critical issues and perspectives. *J. Mol. Catal.* **25**, 51–58 (1984).
7. Paul, R. & Hilly, G. Preparation of an active iron and its application to the semihydrogenation of acetylene derivatives. *Bull. Soc. Chim. Fr.* **6**, 218–223 (1939).
8. Thompson, A. F. & Wyatt, S. B. Partial reduction of acetylenes to olefins using an iron catalyst. *J. Am. Chem. Soc.* **62**, 2555–2556 (1940).
9. Reppe, W. Ethynylation. IV. Reactions of α-alkynols and γ-alkynediols. *Justus Liebigs Ann. Chem.* **596**, 38–79 (1955).
10. Taira, S-I. The Urusibara catalysts. I. Some structural features revealed by X-ray diffraction. *Bull. Chem. Soc. Jpn* **35**, 844–851 (1962).
11. Nitta, Y., Matsugi, S. & Imanaka, T. Partial hydrogenation of phenylacetylene on copper-promoted iron catalyst. *Catal. Lett.* **5**, 67–72 (199
12. Phua, P-H., Lefort, L., Boogers, J. A. F., Tristany, M. & de Vries, J. G. Soluble iron nanoparticles as cheap and environmentally benign alkene and alkyne hydrogenation catalysts. *Chem. Commun.*3747–3749 (2009).
13. Sabatier, P. & Senderens, J. B. Nouvelles méthodes générales d'hydrogénation et de dédoublement moléculaire basées sur l'emploi des métaux divisés. *Ann. Chim. Phys.* **4**, 319–432 (1905).
14. Studt, F. *et al*. Identification of non-precious metal alloy catalysts for selective hydrogenation of acetylene. *Science* **320**, 1320–1322 (2008).
15. Armbrüster, M. *et al*. Pd–Ga intermetallic compounds as highly selective semi-hydrogenation catalysts. *J. Am. Chem. Soc.* **132**, 14745–14747 (2010).
16. Armbrüster, M., Wowsnick, G., Friedrich, M., Heggen, M. & Cardoso-Gil, R. Synthesis and catalytic properties of nanoparticulate intermetallic Ga–Pd compounds. *J. Am. Chem. Soc.* **133**, 9112–9118 (2011).
17. Kovnir, K. *et al*. *In situ* surface characterization of the intermetallic compound PdGa. A highly selective hydrogenation catalyst. *Surf. Sci.* **603**, 1784–1792 (2009).
18. Osswald, J. *et al*. Palladium–gallium intermetallic compounds for the selective hydrogenation of acetylene Part II: Surface characterization and catalytic performance. *J. Catal.* **258**, 219–227 (2008).
19. Osswald, J. *et al*. Palladium–gallium intermetallic compounds for the selective hydrogenation of acetylene Part I: Preparation and structural investigation under reaction conditions. *J. Catal.* **258**, 210–218 (2008).
20. Kovnir, K. *et al*. PdGa and Pd_3Ga_7: Highly-selective catalysts for the acetylene partial hydrogenation. *Stud. Surf. Sci. Catal.* **162**, 481–488 (2006).
21. Kovnir, K. *et al*. A new approach to well-defined, stable and site-isolated catalysts. *Sci. Technol. Adv. Mater.* **8**, 420–427 (2007).
22. Grin, J., Burkhardt, U., Ellner, M. & Peters, K. Refinement of the Fe4Al13 structure and its relationship to the quasihomological homeotypical structures. *Z. Kristal-*

logr. **209**, 479–487 (1994).

23. Gille, P. & Bauer, B. Single crystal growth of $Al_{13}Co_4$ and $Al_{13}Fe_4$ from Al-rich solutions by the Czochralski method. *Cryst. Res. Technol.* **43**, 1161–1167 (2008).
24. Stampfl, C., Ganduglia-Pirovano, M. V., Reuter, K. & Scheffler, M. Catalysis and corrosion: The theoretical surface-science context. *Surf. Sci.* **500**, 368–394 (2002).
25. Seah, M. P. *et al*. Ultra-thin SiO_2 on Si IX: Absolute measurements of the amount of silicon oxide as a thickness of SiO_2 on Si. *Surf. Interface Anal.* **41**, 430–439 (2009).
26. Teschner, D. *et al*. The roles of subsurface carbon and hydrogen in palladium-catalyzed alkyne hydrogenation. *Science* **320**, 86–89 (2008).
27. Popv, P. *et al*. Anisotropic physical properties of the Al13Fe4 complex intermetallic and its ternary derivative Al13(Fe,Ni)4. *Phys. Rev. B* **81**, 184203 (2010).
28. De Smit, E. & Weckhuysen, B. M. The renaissance of iron-based Fischer–Tropsch synthesis: On the multifaceted catalyst deactivation behaviour. *Chem. Soc. Rev.* **37**, 2758–2781 (2008).
29. Danafara, F., Fakhru'l-Razi, A., Salleh, M. A. M. & Biak, D. R. A. Fluidized bed catalytic chemical vapor deposition synthesis of carbon nanotubes—a review. *Chem. Eng. J.* **155**, 37–48 (2009).
30. Powell, C. J. & Jablonski, A. Evaluation of electron inelastic mean free paths for selected elements and compounds. *Surf. Interf. Anal.* **29**, 108–114 (2000).